POWDER-BED BASED 3D-PRINTING OF FUNCTION INTEGRATED PARTS

J. Glasschroeder[1], E. Prager[1], M. F. Zaeh[1]

[1]*iwb Institute for Machine Tools and Industrial Management,*
Technische Universitaet Muenchen, Germany

REVIEWED

Abstract

One big advantage of additive manufacturing technologies is the possibility to create function integrated parts during the manufacturing process. This applies to mechanical functions like movable elements, switches or springs, thermodynamic functions like isolating areas or contour near cooling channels in a part as well as electrical functions like conductive lines and active or passive components. In this paper, recent research results concerning the integration of different elements in a 3D-printed part during the additive manufacturing process and their fields of application are presented. A powder-bed based 3D-printer and polymethyl methacrylate (PMMA) as base material is used for production. The base material is processed by a recoater mechanism to create a plane powder-bed. To enable new functionalities, an automated exhausting mechanism was implemented into the test system. The results of preliminary investigations on integrating attachment elements creating reinforced parts as well as electrical circuits are presented and discussed.

Introduction

In comparison to cutting or forming processes, additive manufacturing is a rather young technology. The first manufacturing machines were presented on the market in the year 1987 [1]. Since then, different technologies and fields of application have evolved. Initially starting with the solidification of plastic materials by a laserbeam, the additive layer manufacturing (ALM) process is now able to handle a huge variety of materials of plastics, metals, ceramics or composites by different modes of solidification [2], [3]. Due to the short production time of for example plastic models, additive manufacturing is well suited to create three dimensional parts with high complexity in a short period of time. Additionally, additively manufactured parts show properties that conventional manufacturing processes can only reach with a lot of additional effort [4]. The field of application of additively manufactured parts is changing from the mere creation of prototypes and illustrative models to an efficient production technology for functional parts in small batches. Hence, this technology can be assigned to the production concept of mass customization [5].

The main application fields of additively manufactured parts are presented in the following diagram (Figure 1).

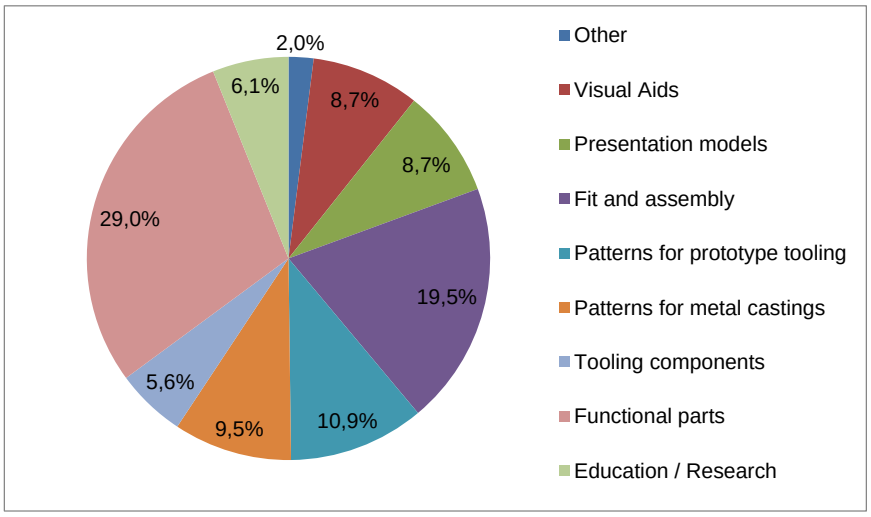

Figure 1: Representation of the main application fields of additive manufactured parts [6]

Generally, ALM processes are still mostly used for creating prototypes or models as well as patterns for the tooling or casting process. Taken individually, creating functional parts is the most important field of ALM processes.

Due to high flexibility, freedom of scope and the possibilities concerning the integration of functions, additive manufacturing has extensive advantages compared to conventional manufacturing technologies [7] and has thereby the potential to revolutionize the way of manufacturing in general [8]. Especially the possibility to integrate different functions in a part is one big advantage which distinguishes this technology from other production technologies.

By taking advantage of this technology, costs for additional work steps can be saved and in consequence production costs for prototypes and small series can be reduced.

State of the art

There are three different main areas of function integration, shown next.

Mechanical functions

Mechanics deals with the motion of parts as well as the cause and effect of forces [9]. Integration of mechanical functions exists if a movement of a body relative to a system or to several other bodies gets improved, simplified or created. Integration of mechanical functions can also mean a change or an improvement of a force or the distribution of forces.

There are several examples in industry and research for realizing mechanical functions using additive manufacturing processes. By not solidifying defined areas of the powderbed, moving elements can be created by removing the loose powder. Switches, hinges or springs can be created by plastic sintering processes without any

additional assembly steps [4]. In comparison to conventional production methods, additional components such as screws, which are needed to fix the part to other elements, can be saved. Other important fields of mechanical functions are parts which fulfill the requirements for “Design for Additive” to improve the distribution of forces in a part [10], [11] as well as lightweight structures or honeycomb structures which reduce the weight of a part retaining similar part properties [12].

Thermodynamic functions

The main target while combining additive manufacturing and thermodynamic functions is to include functions which are based on the exchange or conversion of energy. One example is to adapt the thermal conductivity to the needs of the part by changing the properties of the material. Creating porous materials will raise the thermal insulation due to the enclosed air. Integrated tempering channels help to control the local temperature of the part. Due to the possibilities of almost free forming additive manufacturing gives the chance to integrate for example surface near cooling channels and to optimize them with respect to the existing thermal strains [13]. Shortening the cool-down cycle of the molding tool raises the throughput and makes the injection molding process more efficient.

Electrical functions

The third main field is the integration of electrical functions into a part. Especially for plastic materials, this field opens up a variety of possibilities to create complex parts with new fields of application. The advantages of additive manufacturing technologies, i.e. applying and solidifying material in every layer, offer the possibility to change the material properties, to integrate different materials locally (e.g. conductive materials) or to integrate electrical components. This approach is quite new in comparison to the integration of mechanical and thermodynamic functions and an industrial usage is not known, yet. Several research institutes have published different ways how to realize this aim by using different additive manufacturing technologies.

One attempt is presented by the research group of the University of El Paso in Texas. The creation of conductive paths on an additively manufactured part was shown by Palmer [14]. Medina and Lopes enhanced the system by integrating a dispensing system into a stereolithography machine [15, 16] and demonstrated the functionality by creating a part with an included temperature sensor. Castillo [17] optimized the system and created an accelerometer sensor system integrated into a helmet. The channels and cavities are left open and in a second step filled with a conductive material, in this case by a dispensing system.

The research group of the Lessius Mechelen University College integrated electrical components into parts created by a Fused Deposition Modelling (FDM) system. The

parts are post processed by an aerosol jet printer handling a silver nano ink. Conductive lines as well as electrical components like antennas and resistors can be generated on the surface of the parts [18].

[19] also used the FDM process as a basis for the electrical circuits. By using an additional deposition system (a syringe filled with conductive material), conductive lines are deposited on the building platform next to the standard part material. The cross-sectional dimension of the conductive line is 1,2 mm x 0,8 mm and has a resistance of 0,192 Ω/m.

Apart from the presented main fields, there are a few ancillary areas combining the features of the main fields. In each field, there are a lot of different approaches for integrating functions into parts. Often, only the possibility to integrate additional functions justifies the usage of the ALM technology instead of a conventional production of a part which is often more efficient.

Aims

Especially the technologies using a binder to solidify the materials show a huge potential concerning series production. The binder is deposited via an inkjet printhead on a powder-bed. By using a printhead with multiple modules, the process time can be reduced and consequently the costs for the parts. Furthermore, the building chamber can be designed larger than the one for additive machines using a beam source. The company voxeljet technology AG offers two ALM machines pursuing the aim of mass production. The VX4000 has a building chamber of 4000 x 2000 x 1000 mm and is as such one of the largest ALM machines on the market. To cover the whole width of the platform, the printhead passes one layer twice which leads to a construction progress of 123 l/h. The machine VXC800 shows another approach which allows to produce parts continuously. This offers the possibility to create and unpack parts without stopping the machine.

The technology of binder jetting uses plastic material or sand and was configured to create models for the precision casting or casting cores as well as for creating illustration models for architecture. Poor stability and high porosity of the parts are big disadvantages of this technology. In case of the plastic material PMMA (polymethylmethacrylat), the binder reacts with the powder and solidifies the printed areas. Afterwards, the parts have to stay in the powder-bed for 24 hours until they can be unwrapped. The tensile strength of these parts was measured to be about 4,5 MPa, a post treatment by infiltrating the part with wax or epoxide resin is possible and raises the tensile strength to 28 MPa. Due to the solidification mechanism, the accuracy of this technology is even worse than technologies using a laser-beam.

Even if the efficiency of this technology is much better in comparison to other ALM technologies, the disadvantages prevent an extensive usage of this technology due to minor operational capability. In this paper, three approaches for integrating additional functions into parts, created by a binder jetting technology, are presented. These can make this technology more attractive for other application fields.

Approach

The test rig, a flexible powder-bed based 3D-printer, consists of a process chamber with the dimensions of (LxWxD) 250 x 110 x 95 mm and is equipped with a combined powder feeder and a cylindrical recoater (see Figure 2). A binder is dispensed by an inkjet print head and solidifies the plastic powder locally at the current part cross section. The print head is a Spectra SL128 by the company FUJIFILM Dimatix. With this configuration it is possible to print PolyPorA powder along with the associated binder. After printing, the platform gets lowered by 150 µm. The layer thickness is limited to a minimum of 100 µm due to resolution of the z-axis. Furthermore, up to two print heads can be integrated.

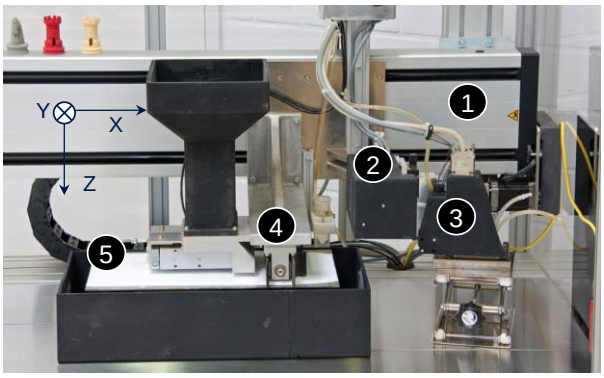

Figure 2: 3D printing test rig; (legend: 1: x-axis, 2: y-axis, 3: print head, 4: powder feeder, 5: powder-bed)

After lowering, a recoater applies a new powder layer. By repeating the steps printing (2), lowering (3) and recoating (1) (see Figure 2) a physical part is generated (see Figure 3).

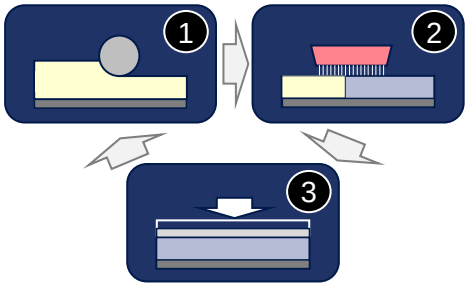

Figure 3: Process steps for the binder jetting ALM process

To be able to create new functions in a part, a new exhausting mechanism was integrated into the test rig. This system enables the local removal of powder to create cavities or channels in one layer. These cavities can be filled with an additional material or components can be placed in there. In most cases, typical components are higher than the thickness of one powder layer. However, a collision with the

recoater must be prevented. So it has to be ensured that the components are placed below the actual powder layer. In combination with the standard ALM process, adding and removing material in one process is possible. The technical realization of the mechanism is shown next.

Exhausting mechanism

Different technologies concerning the handling of powder materials were investigated and evaluated based upon the requirements coming from the process. The system that fulfills these requirements best was a negative pressure exhausting system. To prevent damage to the powder-bed while printing one layer, the exhausting tool has to be placed above the actual powder layer. To be able to reach the powder-bed and to create cavities with up to 20 mm in depth, an additional z-axis (Festo SLTE-50) was integrated into the system. The new axis was placed at the existing y-axis of the test rig, next to the print head. At this position, the x- and y-axis of the test rig can be used to place the new mechanism at any position on the powder-bed. To create a vacuum, a vacuum producer VAD-1/4 was integrated into the system and connected to the exhausting tool on one side and to the compressed air source on the other side by flexible tubes. Between the tool and the vacuum producer, a magnetic valve was implemented to switch the negative pressure. To prevent an early drop of performance of the vacuum producer due to powder congestion, a powder separator was implemented to absorb the loose powder. A pneumatic diagram of the exhausting system as well as an image of the integrated mechanism is presented in figure 4.

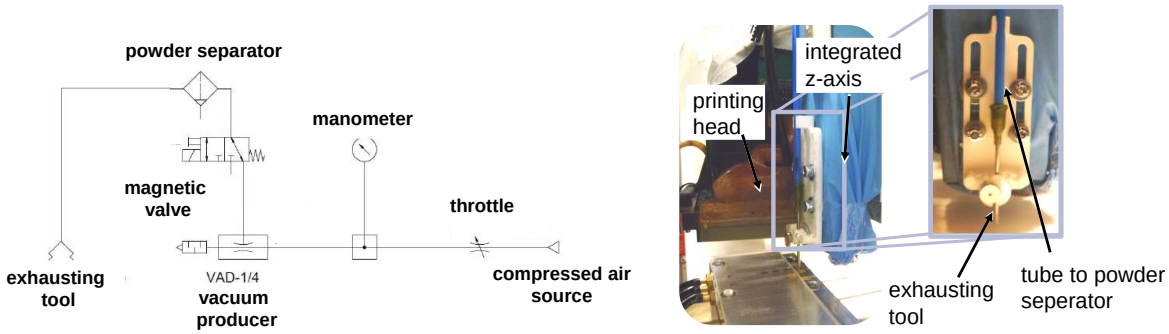

Figure 4: Pneumatic diagram of the implemented exhausting system (left) and image of the integrated system next to the print head (right)

A conventional cannula is used for precise removal of the powder without leaving remains in or next to the cavity. Figure 5 shows channels generated using a cannula with an inner diameter of 1.6 mm and a bended end. Due to the higher thickness, a sufficient negative pressure can be provided to lift the powder particles without clogging the exhausting tool. To create thinner channels, a reduction of the cannula end is necessary. Additionally, the bended tip gets into contact with the powder and also supports the movement of the powder to the opening. Using this system, high

precise cavities can be created with a minimum depth of 0.15 mm. The width of the cavities depends on the used cannula geometry. A test series was performed regarding the accuracy of the exhausting module. Therefore, test specimens as presented in figure 5 (middle) were created and measured by laser microscopy (Keyence VK-9701K) using painted parts. If the parts are not painted the laser-beam passes the transparent powder particles and a surface cannot be recorded. The standard deviation of the created target width is about 50 µm and thus within the technical possibilities, as the average particle diameter of the PMMA powder is about 60 µm.

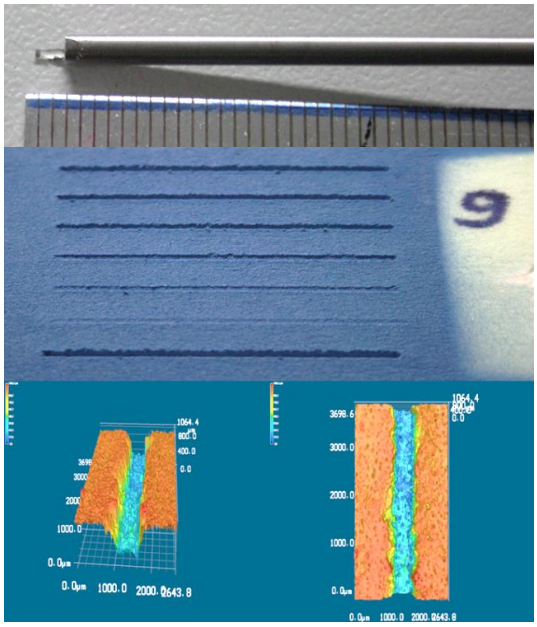

Figure 5: Modified cannula with the bended contact element (top); cavities exhausted by the modified needle with different depth (middle); results of the laser measurement of the exhausted cavities (bottom)

To control the exhausting module, the printing software was extended by a simple numeric control (NC). After printing a layer, the software changes into a separate user interface. The movement commands are created next to the printing data in a separate data file by the user and consist of a sequence of position data as well as height commands for the individual tools. To simplify the removal of powder, in the corresponding areas no binder was printed. Therefore, channels and cavities have to be included already while the part is constructed in a CAD-tool. After starting the exhausting process, the mechanism executes the commands one after the other.

Using this technology, channels and cavities were integrated for different functionalities. The ideas and the results are shown next.

Integrating screw-nuts

As mentioned above, one big disadvantage of the binder jetting technology is the low strength of the parts. In combination with low accuracy and the difficulties to remove the powder in narrow areas, creating mechanical functions like threads or joints by printing the components is hard to realize. To avoid these disadvantages and to benefit from the advantages of the additive manufacturing technology, the exhausting mechanism can be used to implement such mechanical functions.

As an application example, a bolted joint was realized in a part created by the ALM process. This is often necessary due to the fact that the building platform of ALM machines is often smaller than the part which is to be created. The part has to be divided into several sections which are combined in a post-process. Another application is the attachment of other elements (e.g. joining elements) to the part. The proposed solution for this is to integrate a screw nut into the part which then offers a standardized linking possibility.

As the exhausting tool has a cylindrical shape, the cavity has to be larger than the component which is to be integrated. This offset can be calculated (see figure 6) and depends on the outer diameter (r_c) of the needle:

$$s = r_c * (1 - cos45°)$$

Using a cannula with r_c = 0.9 mm, an offset of 0.264 mm at both sides is necessary; therefore the height and the width of the cavity have to be 0,528 mm taller and broader than the component, which is to be integrated.

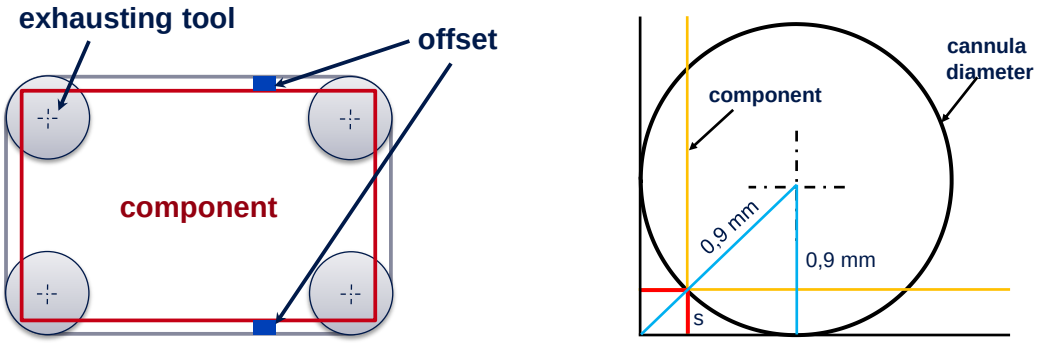

Figure 6: Calculation of the necessary offset of a cavity

An experimental series with a varying offset beginning at 0,5 mm being increased to 0,8 mm indicated that the calculated offset was not sufficient. The component got into contact with the printed part and consequently got out of place. The best results could be generated by using an offset of 0,7 mm (0,35 mm on each side). The additional offset can be explained due to the size of the particles and thus the roughness of the wall surfaces.

After the creation of the cavity, the screw nuts were manually inserted into the part and the process was continued by creating the next powder layer, thereby filling the remaining cavities with powder. To compensate the lost amount of the binder, which evaporated during the exhausting and inserting steps, the actual layer was printed twice. Without this step, a weakening of that layer was noticed.

Pictures of the single steps are shown in the following figure 7.

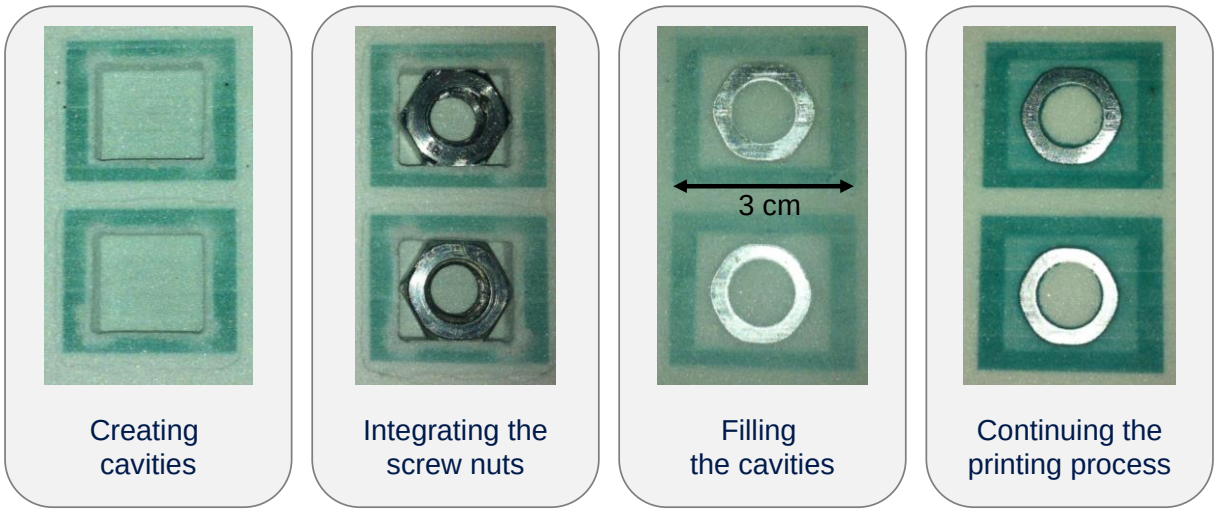

Figure 7: Process steps for integrating screw nuts into an additively manufactured part

The created parts were dried and infiltrated with an epoxide resin (epoxy resin HT2 by the company R&G Faserverbundwerkstoffe GmbH). The same parts were printed without the creation of the cavities to demonstrate the difference of the tensile strength between the two samples. Instead of integrating screw nuts, threads were created manually in the middle of the part. For the tensile test (performed by a Zwick Z100), a mounting support was created which fixes the part on one side and holds a screw on the other side. The tests were performed as proposed in DIN 527-1 with a 5 kN force transducer. To be able to compare the results, the force necessary to pull the screw out of the part was normalized to the length of engagement. Nevertheless, the results showed a broad scattering. Therefore, the average of both methods was calculated. As a result, the average force of the parts whose threads were created directly in the infiltrated material was about 200 N/mm, while parts with integrated screw nuts showed a result of about 430 N/mm. The applied force is distributed to a larger area, which leads to the improvement of the tensile strength.

Creating reinforced elements

Another attempt to eliminate the disadvantage of insufficient mechanical properties of printed parts is a structural functional integration. In this research a reinforcement of the printed parts with fibers of different materials is investigated.

The conventional concept of fiber reinforced plastics implies fibers with diameters below the scale of millimeters. Nevertheless, different approaches demonstrate that the length can vary from a few millimeters (short fibers) to so called endless fibers. To form a fiber matrix compound the following three requirements must be fulfilled:

$$\boldsymbol{\sigma_{fB} > \sigma_{mB}} \qquad \text{(equation 1)}$$

Equation 1 states that the tensile stress at break of the fibers $\boldsymbol{\sigma_{fB}}$ has to be higher than the one of the matrix $\boldsymbol{\sigma_{mB}}$. The same correlation applies for the respective Young's moduli E (E_f = Young's modulus of the fiber and E_m = Young's modulus of the matrix), see equation 2:

$$\boldsymbol{E_f > E_m} \qquad \text{(equation 2)}$$

The third requirement (equation 3) demands that the elongation at break of the matrix (ε_{mB}) is greater than the elongation of the fibers (ε_{fB}):

$$\boldsymbol{\varepsilon_{mB} > \varepsilon_{fB}} \qquad \text{(equation 3)}$$

Two different fibers were considered; the first one was a typical endless carbon fiber with a diameter of approximately 10 µm, which are bundled in a roving. The second fibers had a diameter of several millimeters and were made out of acrylonitrile butadiene styrene (ABS) plastics. Due to their large proportions, the fibers are called inlay structures. Preliminary tests have shown that these materials fulfill equation 1-3 in combination with the existing PMMA matrix.

While the used fibers were higher than one powder layer, the already presented exhausting system was used to create cavities, where the fibers could be deposited in. For conducting tensile test, test specimens according to DIN 50125, type E were produced. In total, six different types of fibers and inlays were used, including two sub-types (figure 8). The purpose of using different shapes of the inlays was to realize the three possible types of connection, traction, form closure and adhesive bonding. Traction was investigated using fibers made of ABS as well as using the carbon fiber roving. The latter was further used for analyzing the connection by adhesive bonding. For investigating the properties of the form closure between matrix and inlay, two different shapes have been developed, each one with a subtype. The diamond-shaped fibers were designed for a better force transmission to the matrix, the wave-shaped fibers to avoid stress peaks in the intersections. The subtypes of both shapes had a hole in the main geometric feature to enlarge the contact surface of inlay and matrix.

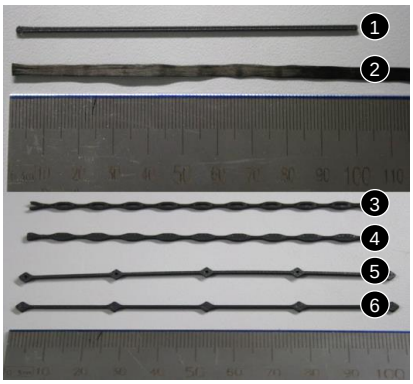

number	type of fiber	material	shape
1	single fiber	ABS	
2	carbon fiber roving	carbon	
3	wave-shaped, hollow	ABS, Inconel	
4	wave-shaped, solid	ABS, Inconel	
5	diamond-shaped, hollow	ABS, Inconel	
6	diamond-shaped, solid	ABS, Inconel	

Figure 8: Different types of fibers; from top to bottom: single fiber, ABS; carbon fiber roving; inlay structure, wave-shaped, hollow; inlay structure, wave-shaped, solid; inlay structure, diamond-shaped, hollow; inlay structure, diamond-shaped, solid

To analyse the effect of the different fibers on the tensile strength of the part, a tensile test using the machine Zwick Z100 was performed. The results are presented next.

Traction

The analysis of the tension bars reinforced with inlays basing on force closure showed a weakening of the test specimens (see figure 9). At first glance traction seemed to be not prevalent. For further investigations of this effect special test specimens (one half of the tension bar) were generated; as a result only one half of the fiber was implemented. Analyzing these parts, a force needed to pull out the inlay could be measured. The traction of the carbon fiber roving was less distinctive than compared to ABS inlays. This behavior can be explained due to the smoother surface of the roving. The apparent weakening of the reinforced tensile bars can be a result of the reduction of the effective cross section due to the necessary cavity for the inlay.

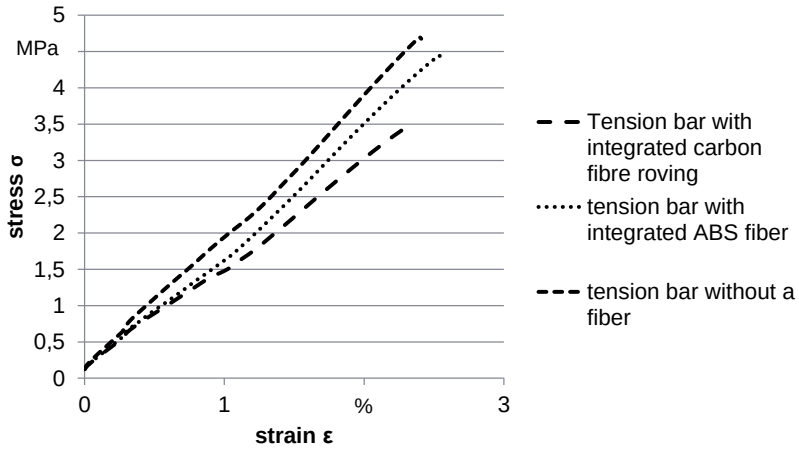

Figure 9: Tensile strength of test specimens reinforced with traction inlays

Form closure

As the test specimens before, the ones reinforced with inlays working with form closure were breaking at lower tensions than without reinforcements. While the inlays based on traction indicate a mostly consistent behaviour, form closure reinforced parts showed massive deviations. One reason for that behavior was found in a chemical incompatibility of the material used for the inlays (ABS) and the binder of the matrix parts (a solvent based on styrene). To prove the anticipated effect, inlays made of Inconel 718 were analysed. These inlays are resistant to the binder and showed the expected effect of an increase of the tensile strength.

Adhesive bonding

The integration of carbon fibers with the principle of adhesive bonds mostly resembles the classic concept of a fiber reinforced plastic part. By infiltrating the test specimens with epoxy resin, a massive gain of strength can be observed. This applies to infiltrated tensile bars without inlays as well as to bars with inlays. Infiltrated parts with carbon fibers showed an increase of the tensile strength compared to parts without the reinforcement of approx. 27 %. A further increase could be realized by integrating Inconel inlay structures. Figure 10 shows the respective values.

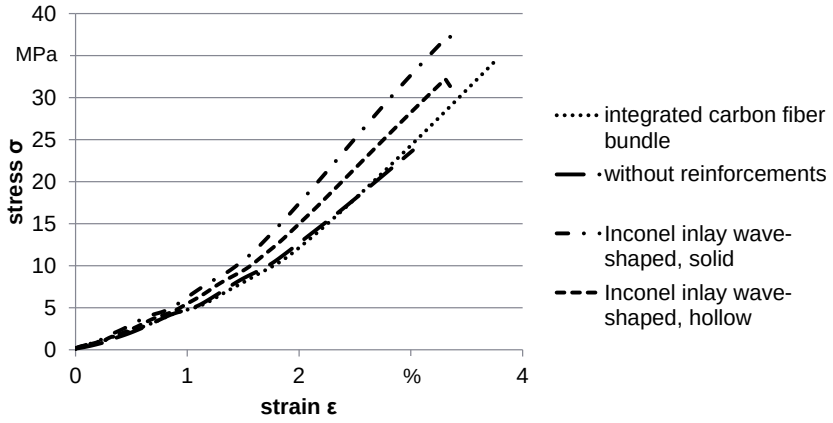

Figure 10: Tensile strength of test specimens reinforced with traction inlays

Conclusion

The reinforcement of parts manufactured by additive processes is possible in general. By employment of fibers made of plastics, the resistance to solvents or physical parameters employed during the process has to be considered. Although the usage of fibers with infiltration showed an increase of the tensile strength, the main drawback is the time-consuming integration and the associated breakage of a pure additive chain of manufacture. An automation of the integration of reinforcing elements would speed up the process and hence increase the efficiency.

Integrating electrical circuits

An electronic circuit is defined as a connection of conductive paths with electrical components [20]. To realize electrical circuits in a part, the standard printing process has to be supplemented by the following steps: integrating electrical components (4), creating conductive paths (5) and connecting both (6), see figure 11.

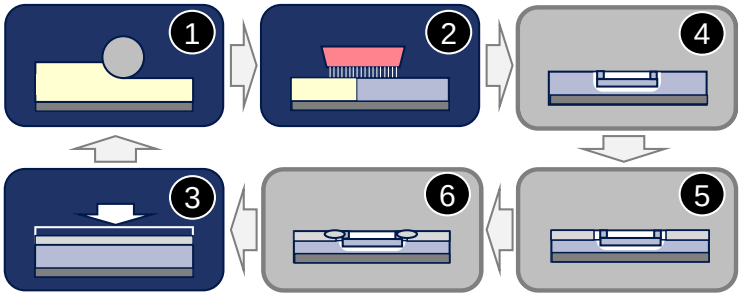

Figure 11: Supplemented process steps for the integration of electrical circuits

As electrical components, resistors in SMT version were chosen due to simpler handling. The smallest purchasable resistor is the 1005 with a width of 200 µm, a length of 400 µm and a height of 130 µm. This part can be deposited on the powder-bed because the generated powder layer is higher than the component. Nevertheless, it can be assumed that the recoater and the powder affect the part whereby the position is changed. For this reason, all components have to be buried in the powder-bed. The approach of integrating resistors is similar to the integration of screw nuts. The exhausting system also allows to pick up parts using a needle with a flat end. A negative pressure of about 0.85 bar can be generated which fixes the part for acceleration. A transportation of the components out of stockage to the right position and depositing them in the created cavity is possible in this way.

For the creation of conductive paths, different materials were investigated and evaluated. Due to the isolating properties of the substrate, they all have in common that an additional material has to be added during the printing process. The materials differ in their state of aggregation (fluid, gas, solid) as well as in their included conductive element (silver, gold, copper, etc.). The fluids can be divided again into fluids with a low viscosity (for example nano silver inks) and fluids with a high viscosity (suspensions, pasts, conductive adhesives, etc.). Fluids with viscosity values lower than 20 mPas are defined as low viscosity fluids as the integrated print head cannot handle fluids of higher viscosity. In general, a higher load of conductive material in the fluid often results in an increase of viscosity [21]. The test rig allows processing of a fluid with a viscosity up to 20 mPas by using the second print head integrated into the system.

Simulation of the 3D-printing process

To compare the operational capability of different fluids (inks, adhesives, suspensions etc.) and to raise the understanding of the effects while depositing a conductive material on a binder soaked powder-bed, a computational fluid dynamics simulation (CFD-simulation) was set up. The geometric modeling of the powder-bed is performed by applying an iterative sphere placing algorithm using the software ANSYS APDL. A powder model with a bulk density of 54 % was created. After depositing the binder on the powder model, a second material with the properties of two different conductive materials was deposited. The first one was a fluid with a viscosity of 20 mPas representing a silver nano ink; the second one was a fluid with a viscosity of 300 mPas representing a conductive adhesive. The simulation demonstrated, that high-viscosity fluids show better results than low-viscosity fluids since the latter get drawn into the powder and form an incoherent conductive structure.

Validation of the simulation results

To validate the results of the simulation, preliminary investigations were performed. First a silver nano ink by the company Xerox was used. This ink has a viscosity of 20 mPas, the load of silver particles is 43 weight percent. The particle size is below 20 nm and the curing temperature is minimum 120 °C. After the building process of several layers with binder, nozzle clogging appeared and led to a black-out of the module. Nevertheless, silver lines with a width of 1 mm were created on the surface of a part. The dried part was sintered in a curing oven at different temperatures starting at 40 °C ranging up to 120 °C. Subsequently to each heating step, the conductivity was tested by a multimeter. Finally, no conductivity could be measured. The conductive adhesive (EPO-TEK E4110, Epoxy Technology Inc.) was deposited manually on the powderbed by using a dispensing system by the company EDF (model 1000XL). After a certain period of time, an electrical conductivity could be measured using a multimeter.

The results of the simulation and the results of the experimental validation are illustrated in figure 12.

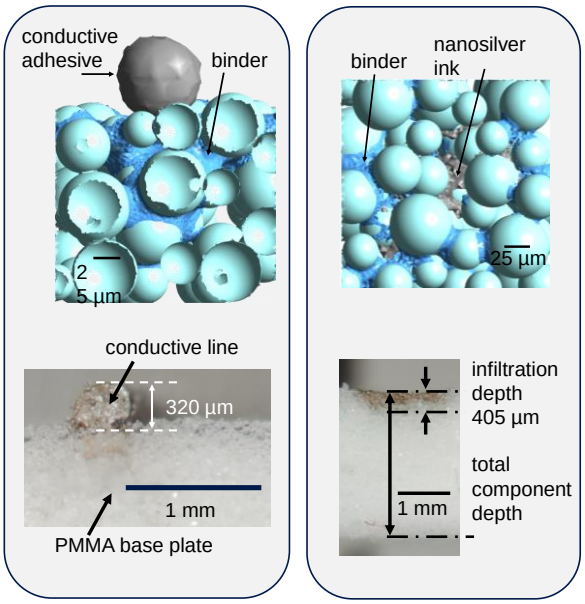

Figure 12: Conductive materials on a powder sample; a conductive adhesive (left), a silver nano ink (right)

Generation of 2D conductive paths

To create conductive lines in a powder-bed, highly viscose materials have to be chosen. To be able to handle these materials, an additional deposition system, a compressed air dispenser, was developed and placed next to the exhausting system at the y-axis. As the boiling temperature of the binder is about 145 °C and the solidification would speed up at higher temperatures, a heat treatment of the integrated conductive paths should be avoided. That is why a two component conductive adhesive, which cures at room temperature, is used. First investigations were made by depositing material continuously on a dried part during the movement of the x-axis. The width of the created lines was approx. 400 µm and the height 300 µm. The current lines are higher than the thickness of one powder layer, so continuing the process without affecting the conductive line or the layer is not possible. Lines with a height below 150 µm should be producible, for example by using thinner needles. As the conductive adhesive requires about 24 hours to solidify at room temperature, an effect of the recoater on the conductive line during the creation of a new powder-bed has to be expected. To avoid an influence of the recoating mechanism, channels are created by using the implemented exhausting mechanism. The channels get filled with conductive material resulting in a total height lower then the normal layer height.

Generation of 3D conductive paths

Besides the creation of conductive paths in one layer, the integrated system offers the possibility to create three-dimensional conductive paths, too. Different methods were investigated to realize vertical conductive lines. The best results were generated by grooving the needle into the powder-bed until it reaches the conductive

line in an underlying layer. During the pull out of the needle, conductive material is emitted until the actual layer is reached. With this method, arbitrarily three-dimensional conductive paths can be created during the process (see figure 13). This allows creating integrated conductive paths in a 3D-printed part. In combination with the integration of electrical components, simple electrical circuits can be created.

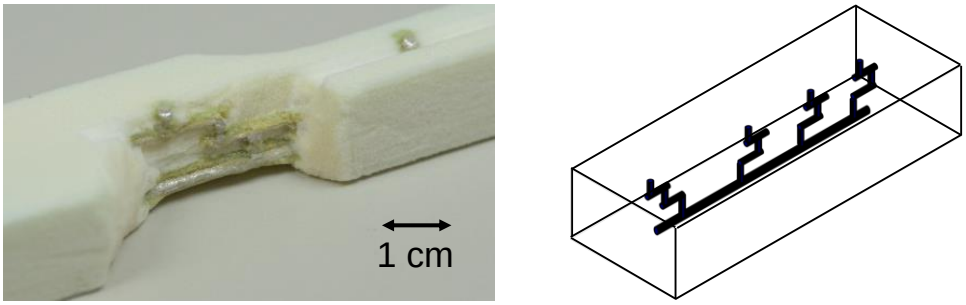

Figure 13: Three-dimensional conductive paths integrated in an additively manufactured part (left), schematic image of the integrated paths (right)

Conclusion and Future Work

The binder jetting technology has high potential for an efficient production of parts. One disadvantage is the low density of the parts. To enlarge the field of application for this technology, the manufacturing system was extended by integrating different functions. The automated exhausting mechanism allows creating cavities or channels which can be filled with an additional material or serve as depositing areas for objects. Two examples for new mechanical functions were presented in this paper. The first attempt was the integration of screw nuts which allows the attachment of other parts; the second attempt was an enforcement of a part while integrating reinforcement elements like carbon fibers. By integrating carbon fibers an increase of 27% in tensile strength is possible. Other use cases can be imagined, for example integrating RFID chips for tracking parts or integrating magnets to fix the plastic part on metal surfaces. Another attempt is to integrate electrical circuits in a part to realize electrical functions. Therefore, a new multi-material system was integrated into the system which allows handling conductive adhesives. In combination with the exhausting mechanism, electrical components as well as conductive paths can be integrated automatically during the regular printing process. Simple electrical circuits can be realized and allow for example the integration of thermocouples into a part.

For future work, the system has to be optimized, especially the compressed air dispenser. The created conductive lines show a very irregular behavior which is due to the imprecise output. A new mechanism based on a screw dispenser should supply material through the nozzle in a more regularly manner. Another aim is to optimize the conductive paths concerning the width and the height of the line. To realize more precise and more complex structures, for example to contact chips or other complex parts, the current conductive paths are too large.

Acknowledgement

The presented studies are amongst others part of the research project “3DAMEEA-3D Additive Manufacturing of Electrical and Electronic Applications” which is funded by the Federal Ministry for Economics and Technology (BMWi).

References

[1] M. Schilling, “Rapid Manufacturing in der Kleinserienproduktion, “ Rtejournal – Forum für Rapid Technologie 5 (2008).

[2] A. Gebhardt, Generative Fertigungsverfahren: Rapid prototyping - rapid tooling - rapid manufacturing, 3rd ed. München: Hanser, 2007.

[3] I. Gibson, D. W. Rosen and B. Stucker, Additive manufacturing technologies: Rapid prototyping to direct digital manufacturing. New York, NY: Springer, 2010.

[4] M. F. Zaeh, Wirtschaftliche Fertigung mit Rapid-Technologien: Anwender-Leitfaden zur Auswahl geeigneter Verfahren. München: Hanser, 2006.

[5] L. Hvam, N. H. Mortensen et al., Product customization, Berlin: Springer, 2008.

[6] T. T. Wohlers, Wohlers report 2014: 3D Printing and Additive Manufacturing State of the Industry: Annual Worldwide Progress Report. Fort Collins, Col: Wohlers Associates, 2014.

[7] G. Reinhart, S. Teufelhart, M. Ott, J. Schilp, “Potentials of Generative Manufactured Components for Gaining Resource Efficiency of Production Facilities,“ in Proceedings of the International Chemnitz Manufacturing Colloquium (ICMC), Chemnitz, Germany, 2010, pp. 703–710.

[8] A. Gebhardt, Understanding additive manufacturing: Rapid prototyping, rapid tooling, rapid manufacturing. Munich, Cincinnati: Hanser Publishers, 2012.

[9] H. Goldstein, C. P. Poole and J. L. Safko, Klassische Mechanik, 3rd ed. Weinheim: Wiley-VCH, 2006.

[10] S. Teufelhart and G. Reinhart, “Optimization of strut diameters in lattice structures,” in 23th Annual Solid Freeform Fabrication Symposium, Austin, TX, USA, 2012, pp. 719–733.

[11] C. Emmelmann, P. Sander, J. Kranz, and E. Wycisk, “Laser Additive Manufacturing and Bionics: Redefining Lightweight Design,” Physics Procedia, vol. 12, pp. 364–368, 2011.

[12] G. Reinhart, S. Teufelhart, and F. Riß, “Examination of the Geometry-dependent Anisotropic Material Behavior in Additive Layer Manufacturing for the Calculation of Mesoscopic Lightweight Structures,” in Fraunhofer Direct Digital Manufacturing Conference 2014, 2012.

[13] M. Ott; S. Teufelhart; F. Riß, “Innovationen durch den Einsatz additiver Fertigungsverfahren, “ emobilitytec (2013) 3, pp. 52-56.

[14] J. A. Palmer, D. Davis, P. Gallegos, P. Yang, B. D. Chavez, F. R. Medina, and R. Wicker, “Stereolithography: A Basis for Integrated Meso Manufacturing,” in 16th Annual Solid Freeform Fabrication Symposium, Austin, TX, USA, 2005, pp. 476–483.

[15] F. R. Medina, A. Lopes, A. Inamdar, R. Hennessey, J. A. Palmer, B. D. Chavez, D. Davis, P. Yang, P. Gallegos, and R. Wicker, “Hybrid Manufacturing: Integrating Direct Write and Stereolithography,” in 16th Annual Solid Freeform Fabrication Symposium, Austin, TX, USA, 2005, pp. 39–49.

[16] A. Lopes, M. Navarrete, F. R. Medina, J. A. Palmer, E. MacDonald, and R. Wicker, “Expanding Rapid Prototyping for Electronix Systems Integration of Arbitrary Form,” in 17th Annual Solid Freeform Fabrication Symposium, Austin, TX, USA, 2006, pp. 644–655.
[17] S. Castillo, D. Muse, F. R. Medina, E. MacDonald, and R. Wicker, “Electronics Integration in Conformal Substrates Fabricated with Additive Layered Manufacturing,” in 20th Annual Solid Freeform Fabrication Symposium, Austin, TX, USA, 2009, pp. 730–737.
[18] F. Vogeler, W. Verheecke, A. Voet, and H. Valkenaers, “An Initial Study of Aerosol Jet® Printed Interconnections on Extrusion-Based 3D-Printed Substrates,” Strojniški vestnik - Journal of Mechanical Engineering, vol. 59, no. 11, 2013.
[19] D. Periard, E. Malone, and H. Lipson, “Printing Embedded Circuits,” in 18th Annual Solid Freeform Fabrication Symposium, Austin, TX, USA, 2007.
[20] H. Wupper and U. Niemeyer, Elektronische Schaltungen 1: Grundlagen, Analyse, Aufbau.
[21] H.-H. Lee, K.-S. Chou, and K.-C. Huang, “Inkjet printing of nanosized silver colloids,” Nanotechnology, vol. 16, no. 10, pp. 2436–2441, 2005.